Experimental assessment of solute dispersion in stratified porous media

Kurasawa, Tomoki
Suzuki, Mariko
Inoue, Kazuya

(Citation)
Hydrological Research Letters,14(4):123-129

(Issue Date)
2020

(Resource Type)
journal article

(Version)
Version of Record

(URL)
https://hdl.handle.net/20.500.14094/90007862

Hydrological Research Letters **14**(4), 123–129 (2020)
Published online in J-STAGE (www.jstage.jst.go.jp/browse/hrl). DOI: 10.3178/hrl.14.123

Experimental assessment of solute dispersion in stratified porous media

Tomoki Kurasawa, Mariko Suzuki and Kazuya Inoue
Graduate School of Agricultural Science, Kobe University, Japan

Abstract:

The objective of this paper is to evaluate effects of stratified porous formation on solute dispersion using two-dimensional laboratory tracer tests. An image analysis technique was used to analyze the solute dispersion processes and quantify the dispersivity and behaviors of forward and backward tails of solute plumes. Longitudinal dispersivity estimates for the stratified porous media increased with travel distance and are in reasonable agreement with previous work. Moreover, in all of the stratified cases the transverse dispersivity exhibited a similar trend which decayed with travel distance. The summary of dispersivities estimated from this study and previous studies suggests that if both degree of heterogeneity and scale for stratified and randomly heterogeneous porous media are similar, the longitudinal dispersivity is larger in stratified media than in randomly heterogeneous media. In order to quantify behaviors of forward and backward tails, we defined the travel distances x_{05} and x_{95} corresponding to the 5th and 95th percentiles, respectively, of the cumulative concentrations in the longitudinal direction, and found that the distance between x_{05} and x_{95} spread out linearly in the stratified cases.

KEYWORDS solute dispersion; stratified porous media; laboratory-scale experiments; image analysis technique; dispersivity; solute plume tails

INTRODUCTION

Natural soils and aquifers often possess very complex spatial patterns of hydraulic conductivity (Nakagawa *et al.*, 2012; Zinn *et al.*, 2004), leading to dispersive mixing of solutes. Solute dispersion is one of the key factors in understanding the fate and transport of solute contaminants within groundwater. Therefore, quantifying the effect of heterogeneous structure on the strength of the dispersion process is of significance. Most studies using mathematical, numerical, geostatistical, or stochastic methods have investigated the relationship between heterogeneous structure and the dispersion parameters such as the dispersivity and the dispersion coefficient (Beaudoin and de Dreuzy, 2013; Dagan, 1984; Fernàndez-Garcia and Gómez-Hernández, 2007; Fiori *et al.*, 2010; Gelhar and Axness, 1983). In particular, solute dispersion in stratified porous media has been studied frequently (Bolster *et al.*, 2011; Gelhar *et al.*, 1979; Güven *et al.*, 1984; Mercado, 1967; Zavala-Sanchez *et al.*, 2009) because natural sandy aquifers often exhibit geological stratification characterized by a much larger horizontal than vertical correlation length. These studies have provided the foundation for the quantification of the dispersivity and the dispersion coefficient within stratified media. Compared with the large number of theoretical and numerical works, field tracer experiments are rather scarce. One cause for this might be the difficulty of carrying out field tests on a routine basis.

Alternatively, laboratory tracer experiments have been widely used to understand the influence of various factors on solute transport within porous media (Chao *et al.*, 2000; Danquigny *et al.*, 2004; Fernàndez-Garcia *et al.*, 2002; Heidari and Li, 2014; Silliman and Simpson, 1987; Ye *et al.*, 2015; Zhang *et al.*, 2019). These experiments have an advantage that the physical and chemical properties in the porous media are well defined. Several laboratory experiments were coupled with image analysis techniques that permitted, through the use of specific procedures, the estimation of the solute concentration in the test aquifer without the use of invasive instruments (Citarella *et al.*, 2015; Jaeger *et al.*, 2009; McNeil *et al.*, 2006; Ursino *et al.*, 2001; Zinn *et al.*, 2004). It has been noted that a number of laboratory tests in homogeneous and two- and three-dimensional (2D and 3D, respectively) random hydraulic conductivity fields are available from the literature (Chao *et al.*, 2000; Fernàndez-Garcia *et al.*, 2002, 2005b; Inoue *et al.*, 2016a; Levy and Berkowitz, 2003); however, laboratory experiments on stratified formations are very few in comparison to those on homogeneous and random fields (Inoue *et al.*, 2016b). Although Inoue *et al.* (2016b) investigated scale-dependence of longitudinal dispersivity in stratified porous formations and the relationship between the dispersivity and the degree of heterogeneity, they did not evaluate effects of stratified structure (i.e. the contrast between layer thickness and hydraulic conductivity) on solute dispersion.

The objective of this paper is to examine how stratified nature, particularly the contrast between layer thickness and hydraulic conductivity, may control solute dispersion. We consider one of the simplest models of stratified formation, namely a step-function model where the heterogeneity consists of a succession of two porous materials in serial order. For this model, two-dimensional laboratory tracer experiments were conducted and an image analysis technique was used to analyze the solute dispersion processes. Furthermore, because the behaviors of the forward and backward

Correspondence to: Kazuya Inoue, Graduate School of Agricultural Science, Kobe University, 1-1 Rokkodai, Nada-ku, Kobe, Hyogo 657-8501, Japan. E-mail: mornel@kobe-u.ac.jp

Received 1 June, 2020
Accepted 30 July, 2020
Published online 7 October, 2020

tails of solute plumes are of particular importance due to their potential for groundwater contamination, we also thereby present an approach to quantify the behaviors of forward and backward plume tails.

MATERIALS AND METHODS

Experimental apparatus

The laboratory experiments were performed in a sandbox of internal dimensions 200 cm × 80 cm × 3 cm (length × height × width, respectively). The design of the sandbox is illustrated in Figure 1. Constant head spill reservoirs connected to the upstream and downstream ends of the tank were used to control the flow through the outer boundaries of the sand pack. At the front side, a window with a 3-cm thick glass pane provided an opportunity for visual observations. At the rear side, an acrylic plate permitted the introduction of 10 pressure measurement ports as well as 8 solute injection ports (labeled a–h). The upstream and downstream ends of the sandbox were separated from the porous medium by thin meshes with hydraulic conductivity lager than that of the porous materials.

Porous media

In our experiments, three different types of sorted silica sands (S1, S2 and S3) with differing grain sizes were employed. The hydraulic conductivity of each sand was determined in the following steps. Firstly, a one-dimensional column was packed with each sand. Under a steady-state condition, flow rate and hydraulic gradient were measured, and Darcy's law was used to calculate the hydraulic conductivity. The relevant properties of the sands are given by Table SI.

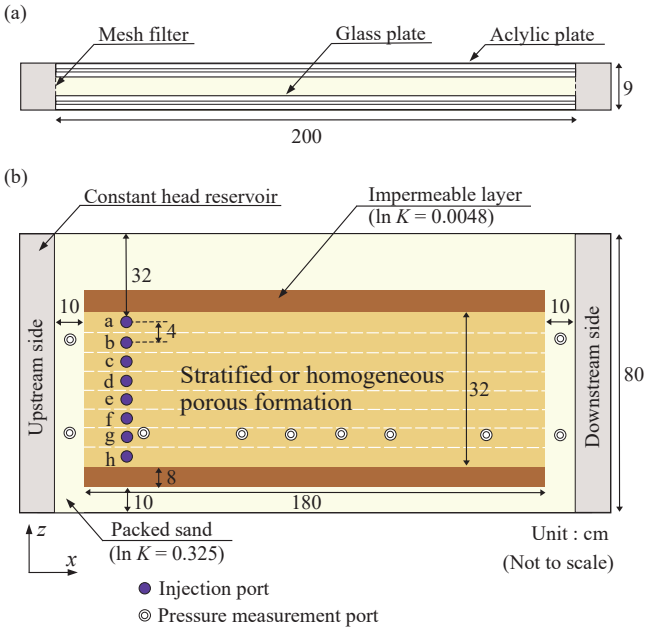

Figure 1. The design of the sandbox: (a) Top view; and (b) front view with injection and pressure measurement ports lay-out. ln K denotes the natural logs of hydraulic conductivity

Three stratified structures were constructed within the sandbox, labeled as the A-4, A-16, and B-4 cases (Table I). These stratified cases are step-function models. As illustrated in Table I, A-4 had eight layers of 4-cm thickness, including four high- and four low-conductivity layers (composed of S3 and S2 sands, respectively); whereas A-16 had two layers of 16-cm thickness, including one each of high- and low-conductivity layers (S3 and S2, respectively). B-4 had eight layers of 4-cm thickness, including four high- and four low-conductivity layers (S3 and S1, respectively). Note that while A-4 and B-4 had the same thickness and number of layers, there were differences in hydraulic conductivity contrast and heterogeneity between these cases. Also, A-4 and A-16 had the same hydraulic conductivity contrast and heterogeneity, whereas there were the differences in the thickness and number of layers. Thus, compared with A-4, for A-16 mass transfer among high and low conductivity layers due to transverse dispersion hardly occurs. Here, hydraulic conductivity contrast C and the heterogeneity $\sigma^2_{\ln K}$ (the variance of ln K) are calculated by:

$$C = \frac{K_h}{K_l} \tag{1}$$

$$\sigma^2_{\ln K} = \frac{1}{n}\left(\sum_{i=1}^{n} (\ln K_i)^2 - n(\ln M)^2\right) \tag{2}$$

where K_h and K_l are the hydraulic conductivities in the high- and low-conductivity layers of a stratified medium, n is the number of layers, K_i is the hydraulic conductivity of layer i, and M is the geometric mean of hydraulic conductivity. The hydraulic conductivity contrast and the heterogeneity of each case are also shown in Table I. The extent of hydraulic conductivity variation differs significantly in different natural aquifers ($\sigma^2_{\ln K} = 0.14 - 4.5$) (Boggs *et al.*, 1992; Mackay *et al.*, 1986; Sudicky, 1986). In this study, $\sigma^2_{\ln K}$ values of stratified formations were relatively small ($\sigma^2_{\ln K} = 0.113 - 0.762$). To verify the reliability of the experimental device, experiments in homogeneous packing of S3 were also performed using the sandbox in Figure 1 and a one-dimensional column that had a 5-cm internal diameter and a length L = 30 cm, and we compared the longitudinal

Table I. Summary of experimental cases

Schematic[a]	Cases	Thickness of layers (cm)	K contrast C (–)	Heterogeneity $\sigma^2_{\ln K}$ (–)
	A-4	4	1.96	0.113
	A-16	16	1.96	0.113
	B-4	4	5.72	0.762

[a] S1 (K = 0.0341 cm/s)
S2 (K = 0.0996 cm/s)
S3 (K = 0.195 cm/s)

dispersivities obtained from these devices.

Sand packing was carried out under saturated conditions, with the sand being poured through at least 2 cm of water in order to avoid air entrapment. The sands of concern were packed in 2-cm or 4-cm layers using narrow metal dividers in order to establish sharp contacts between regions of different sands. The dividers were gradually removed as packing progressed.

Experimental procedure and image acquisition

The dye Brilliant Blue FCF, which is a non-toxic compound and consequently relatively safe to handle (Flury and Flühler, 1994), was chosen as a tracer for image analysis. After establishing steady-state flow conditions, a dilute Brilliant Blue FCF solution with a concentration of 0.2 mg/L was injected. Here, the eight injection ports (a–h) along the transverse line were used in order to encounter the spatial heterogeneity of the entire stratified medium. This concentration was chosen so as to minimize density effects yet still provide a sufficiently broad range over which meaningful concentration measurements could be made. For all cases, light sources and a digital camera were placed in front of the sandbox filled with silica sands. During the experiments, the digital camera captured a series of red, green, and blue (RGB) images of the solute plume (Figure S1(a)). All images consisted of 800 (length) × 600 (height) pixels with a resolution of around 4 pixels/cm.

Image analysis

For each image, each pixel displays a color based on its RGB combination. Thus, it is possible to divide the three color channels in order to perform a transformation on each image, resulting in three different images in gray scale. In this manner, each pixel may assume integer values from 0 (black) to 255 (white), thereby enabling the measurement of the pixel intensity of the whole image in each channel. In this study, the three colors channels were separated and only red values were taken into consideration. The dye concentration was correlated with red color intensity using a calibration procedure consisting of the following steps: (1) injection of a solute plume at a known concentration in the porous medium; (2) acquisition of an image; (3) restart from step (1) with a new solution concentration. This procedure was performed for different concentrations in order to obtain adequate calibration curves. The red value of the dye relates to the size of the sand grain and the lighting condition as well as the dye concentration. Therefore, for each experimental case, each sand type was characterized by a unique calibration curve (as shown in Figure S2) and these curves were used to determine solute concentration maps (Figure S1(b)).

Evaluation of dispersivities from spatial moments

Spatial moment analysis has been widely used for the quantification of solute spreading in transport problems (Adams and Gelhar, 1992; Freyberg, 1986; Inoue *et al.*, 2016b; Kurasawa and Inoue, 2019). In two-dimensional experiments, the *ij*th spatial moment of a concentration distribution M_{ij} is defined by:

$$M_{ij}(t) = \int_{-\infty}^{\infty}\int_{-\infty}^{\infty} c(x,z,t)x^i z^j dxdz \tag{3}$$

where $c(x, z, t)$ is the solute concentration, t is the time, x (horizontal) and z (vertical) are spatial Cartesian coordinates, and i and j are nonnegative integers. The centers of mass of the solute plume in the x and z directions are calculated by:

$$x_G(t) = \frac{M_{10}(t)}{M_{00}(t)} \tag{4}$$

$$z_G(t) = \frac{M_{01}(t)}{M_{00}(t)} \tag{5}$$

where x_G and z_G are the centers of mass of the tracer plume in the x and z directions, respectively. Using Equations (4) and (5), the second moment about the center of mass defines a spatial covariance tensor (Freyberg, 1986; Inoue *et al.*, 2016b; Kurasawa and Inoue, 2019):

$$\begin{aligned}\sigma_{ij}(t) &= \begin{pmatrix}\sigma_{xx}(t) & \sigma_{xz}(t)\\ \sigma_{zx}(t) & \sigma_{zz}(t)\end{pmatrix}\\ &= \begin{pmatrix}\dfrac{M_{20}(t)}{M_{00}(t)} - (x_G(t))^2 & \dfrac{M_{11}(t)}{M_{00}(t)} - x_G(t)z_G(t)\\ \dfrac{M_{11}(t)}{M_{00}(t)} - z_G(t)x_G(t) & \dfrac{M_{02}}{M_{00}} - (z_G(t))^2\end{pmatrix}\end{aligned} \tag{6}$$

where σ_{ij} is the second moment about the center of mass. The longitudinal and transverse dispersivities are defined as (Bear, 1972):

$$A_L(\xi_c, t) = \frac{1}{2}\frac{\sigma_{xx}(t)}{\xi_c(t)} \tag{7}$$

$$A_T(\xi_c, t) = \frac{1}{2}\frac{\sigma_{zz}(t)}{\xi_c(t)} \tag{8}$$

where A_L and A_T are the longitudinal and transverse dispersivities, and ξ_c is the travel distance of the center of mass of the tracer plume in the mean flow direction (x direction).

RESULTS AND DISCUSSION

Longitudinal dispersivity

The longitudinal dispersivity values for homogeneous packing (S3) of the sandbox in Figure 1 were within a range of 0.075–0.13 cm. This result is in good agreement with the value (A_L = 0.072 cm) for the one-dimensional column, indicating reliability of the experimental device. Longitudinal dispersivity of the stratified cases as a function of travel distance of the center of mass is shown in Figure 2(a) together with the analytical solution provided by Mercado (1967). Analysis by Mercado (1967) of horizontal displacement through a stratified aquifer illustrates some effects of variation of the hydraulic conductivity in the vertical direction. Mercado's analytical solution of the longitudinal dispersivity is given as (Gelhar *et al.*, 1979; Mercado, 1967):

$$A_L = \frac{1}{2}\left(\frac{\sigma_K}{\overline{K}}\right)^2 \overline{x} \tag{9}$$

where σ_K is the standard deviation of hydraulic conductivity, $\overline{K}$ is the average value of hydraulic conductivity, and $\overline{x}$ is the mean travel distance. Note that the dispersivity calculated by Mercado's solution is proportional to the variance of the hydraulic conductivity and grows indefinitely with

travel distance. Cases A-4 and A-16 had the same value of longitudinal dispersivity computed from Equation (9) because these cases had the same values of σ_K and $\bar{K}$.

As can be seen from Figure 2(a), longitudinal dispersivity increased with travel distance in the three stratified cases. As expected from previously published studies (Gelhar *et al.*, 1992), longitudinal dispersivities from heterogeneous porous media (i.e. the stratified cases) exhibited scale-dependent behaviors. The scale-dependence of A_L also provides evidence that the scale-dependence of longitudinal dispersivity can be observed under 2D controlled laboratory conditions. Cases A-4 and A-16 had the same values for hydraulic conductivity contrast and heterogeneity, while longitudinal dispersivity estimates for A-16 were slightly higher than those for A-4. This suggests that the mass transfer driven by transverse dispersion between the high- and low-conductivity layers was larger for A-4 than for A-16 due to the relatively small layer thickness, leading to relatively small longitudinal (x-direction) spreading of the tracer plume. Pickens and Grisak (1981) reached a similar conclusion from their review of previous field tests and from longitudinal dispersivity values obtained in their own tests. Thus, our results support the conclusion by Pickens and Grisak (1981). Although A-4 and B-4 had the same layer thickness, their longitudinal dispersivities exhibited different scale-dependent behaviors. This discrepancy is attributed to the difference in heterogeneity (i.e. the hydraulic conductivity contrast) between the two cases.

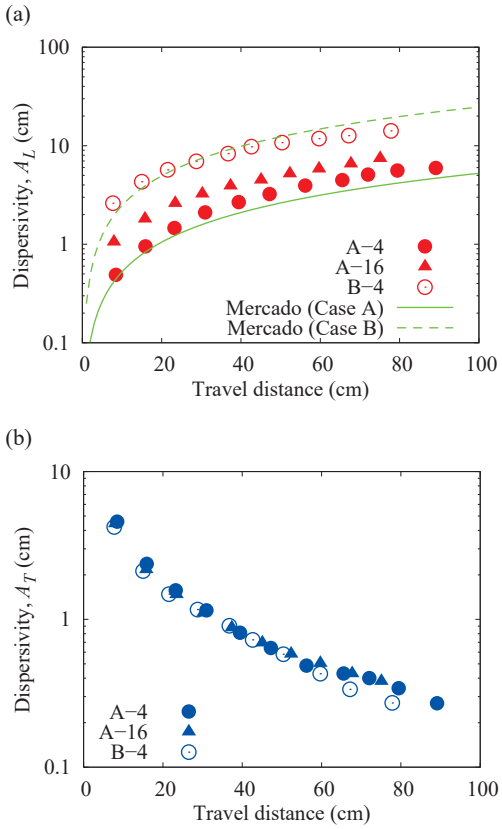

Figure 2. Dispersivities as a function of travel distance of the center of mass: (a) Longitudinal dispersivity; and (b) transverse dispersivity. Solid symbols represent Case A-4 (circles) and A-16 (triangles), and open symbols represent B-4 (circles). Solid and dashed lines correspond to the dispersivity calculated by Equation (9) for Case A and B, respectively

As shown in Figure 2(a), longitudinal dispersivity values are in reasonable agreement with the analytical solution for all stratified cases. This result demonstrates the validity of our experiment. As mentioned above, the dispersivity estimated from Mercado's solution grows indefinitely with scale, whereas in general, longitudinal dispersivity approaches a constant value at large distance scales (Fernàndez-Garcia *et al.*, 2005a). Although at the travel distance of our experiments the results of A_L agree with Mercado's solution, the dispersivities obtained from experiments versus Mercado's solution may exhibit different scale-dependent behavior at relatively large scales. Further experimental studies for larger scale are needed to demonstrate the practical capacity of Mercado's analytical solution.

Transverse dispersivity

Transverse dispersivity as a function of travel distance is shown in Figure 2(b). In all cases, this parameter shows a similar trend which decays with increasing travel distance. To explain this behavior shown in Figure 2(b), Figure 3 shows values of σ_{zz} as a function of travel distance. In all cases, σ_{zz} remains approximately constant. This is because σ_{zz}, which is the mean-square displacement in the transverse direction, depends on the initial source size in the transverse direction (i.e. the eight-point injection), and in the stratified cases, hydraulic conductivity of the porous media varied only in the vertical direction (i.e. z direction) and did not significantly change solute distribution in the z direction. As a result, the behavior of σ_{zz} led to the aforementioned behavior of A_T which was computed by Equation (8).

Comparison of dispersivities estimated from this study and earlier works

To put our work in the context of others and to understand the influence of various factors (i.e. the heterogeneity, scale, flow configuration and spatial variability of the hydraulic conductivity) on the dispersivities, Table II shows a summary of the dispersivities and the factors for this

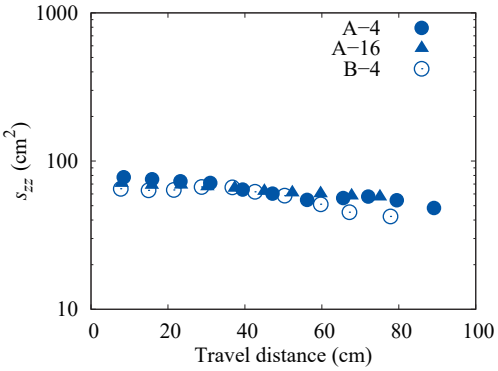

Figure 3. The mean-square displacement in the transverse direction σ_{zz} as a function of travel distance of the center of mass

Table II. Summary of longitudinal and transverse dispersivities obtained from laboratory-scale experiments in heterogeneous porous media

Longitudinal dispersivity A_L (cm)	Transverse dispersivity A_T (cm)	Heterogeneity $\sigma^2_{\ln K}$ (–)	Scale[a] (cm)	Flow Configuration	Spatial variability of K	Ref.[b]
6.52–14.2	0.270–0.382	0.113–0.762	75.1–89.1	Uniform flow	Stratified	1
0.187–0.594	—	1.81	25.4–43.2	Radial flow	2D random	2
12	—	1.81	219.6	Uniform flow	2D random	2
0.14–6.76	—	1.47	21–100	Radial flow	2D random	3
0.92–6.4	0.063–1.4	0.36–3.6	26.5–47.8	Uniform flow	Stratified	4
0.138–1.90	0.0111–0.638	0.0741–0.307	40.4–56.0	Uniform flow	2D random	5
4.6	0.019	0.24	380	Uniform flow	2D random	6

[a] Scale represents travel distance of solute plume

[b] 1. This study, 2. Chao *et al.* (2000), 3. Fernández-Garcia *et al.* (2002), 4. Inoue *et al.* (2016b), 5. Kurasawa and Inoue (2019), 6. McNeil *et al.* (2006)

study and earlier laboratory-scale experiments in heterogeneous porous media. For our work, the heterogeneity values have a relatively low range and scales (i.e. travel distances) cover a middle range. Compared with Inoue *et al.* (2016b), A_L values in our study were larger overall. This is mostly due to the larger travel distances. Moreover, for similar heterogeneity values and scales A_L values of stratified porous media tend to be larger compared to those of randomly heterogeneous porous media. This suggested that if both heterogeneity value and scale for stratified and randomly heterogeneous porous media are similar, the longitudinal dispersivity is larger in stratified media than in randomly heterogeneous media.

As expected from previously published studies (Gelhar *et al.*, 1992), in all studies values of transverse dispersivity are 1–2 orders of magnitude smaller than values of longitudinal dispersivity. Table II also shows that transverse dispersivity varied over several orders of magnitude. Compared with the data of longitudinal dispersivity, those of transverse dispersivity were more limited and did not imply any significant trend (Gelhar *et al.*, 1992). In particular, and as mentioned previously, although transverse dispersivity estimates depend on initial source size, the overall effect of source size on transverse dispersivity is not yet clear based on the studies summarized in Table II. Thus, there is a need for further development in understanding the effect of source size on a transition of the transverse dispersivity.

Forward and backward tails

In order to quantify behaviors of forward and backward tails, we defined the travel distances x_{05} and x_{95} corresponding to the 5th and 95th percentiles, respectively, of the cumulative concentrations in the x direction (Figure S3). Thus, x_{05} and x_{95} reflected travel distances of the fastest (forward) and slowest (backward) portions of a tracer plume (Figure S4). In order to quantify spreading of the solute plume, $x_{05–95}$, which is the distance between x_{05} and x_{95}, was also calculated. Further discussion about $x_{05–95}$ is included the supplementary material (Text S1). $x_{05–95}$ as a function of displacement distance is shown in Figure 4. This figure shows that $x_{05–95}$ increases linearly with travel distance. This indicated that for step-function models, forward and backward tails spread out linearly in the longitudinal direction.

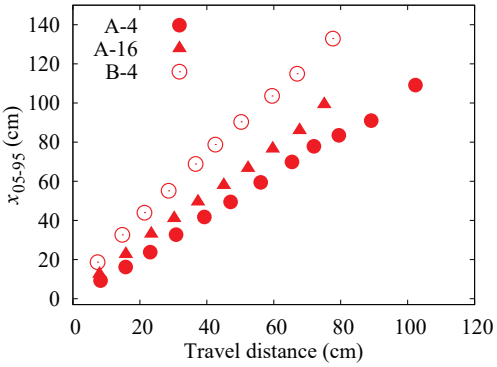

Figure 4. Distance between x_{05} and x_{95} versus travel distance of center of mass. x_{05} and x_{95} correspond to the 5th and 95th percentiles, respectively, of the cumulative concentrations

CONCLUSIONS

The purpose of this study was to evaluate the effects of the stratified structure on solute dispersion. Laboratory-scale tracer experiments were conducted in the three stratified porous media where the heterogeneity consisted of a succession of two porous materials in serial order (i.e. step-function model). An image analysis technique was used to analyze the solute dispersion processes and the behaviors of the forward and backward tails. The main conclusions from this study are summarized as follows:

1. Longitudinal dispersivity increased with travel distance in the stratified porous media. This result provides evidence that the scale-dependence of longitudinal dispersivity in heterogeneous porous media can be observed in two-dimensional laboratory sandbox.
2. Longitudinal dispersivity estimates were in reasonable agreement with the analytical solution for the stratified porous media, demonstrating the validity of our experi-

ment.

3. In all three stratified porous media cases, transverse dispersivity exhibited a similar trend of decay with travel distance. This is because transverse dispersivity depends on the initial source size in the transverse direction.
4. The summary of longitudinal and transverse dispersivities estimated from this study and previous studies indicate that when both heterogeneity and scale for stratified and randomly porous media are similar, the longitudinal dispersivity is larger in stratified media than in randomly heterogeneous media.
5. We defined the travel distances x_{05} and x_{95} corresponding to the 5th and 95th percentiles of the cumulative concentrations in the longitudinal direction, thus reflecting the travel distances of the fastest and slowest portions of a tracer plume, respectively. We found that in the step-function models, forward and backward tails spread out linearly in the longitudinal direction.

ACKNOWLEDGMENTS

This work was supported by JSPS KAKENHI Grant Numbers JP19H03074, JP20J10801.

SUPPLEMENTS

Text S1. Evaluation of forward and backward tails

Figure S1. Snapshots of solute plume: (a) plume image; and (b) concentration map

Figure S2. Calibration curves: (a)A-16; and (b) B-4. Case A-16 has two layers composed of S3 and S2 sands, whereas Case B-4 has eight layers composed of S3 and S1 sands

Figure S3. Illustration of forward and backward tails: (a) example of concentration profiles of a solute plume in the x-direction; and (b) a snapshot of solute distribution. x_{05} and x_{95} are the travel distances corresponding to the 5th and 95th percentiles, respectively, of the cumulative concentrations in the x direction

Figure S4. x_{05} and x_{95} as a function of travel distance of the center of mass: (a) A-4; (b) A-16; and (c) B-4. x_{05} and x_{95} are the travel distances corresponding to the 5th and 95th percentiles, respectively, of the cumulative concentrations in the x direction. The red lines represent travel distance of the center of mass (x_G)

Table SI. Properties of the test sands

REFERENCES

Adams EE, Gelhar LW. 1992. Field study of dispersion in a heterogeneous aquifer: 2. Spatial moment analysis. *Water Resources Research* **28**: 3293–3307. DOI: 10.1029/92WR01757.

Bear J. 1972. Dynamics of Fluids in Porous Media. American Elsevier Publishing Company; NY; 579–664.

Beaudoin A, de Dreuzy J-R. 2013. Numerical assessment of 3-D macrodispersion in heterogeneous porous media. *Water Resources Research* **49**: 2489–2496. DOI: 10.1002/wrcr.20206.

Boggs JM, Young SC, Beard LM, Gelhar LW, Rehfeldt KR, Adams EE. 1992. Field study of dispersion in a heterogeneous aquifer: 1. Overview and site description. *Water Resources Research* **28**: 3281–3291. DOI: 10.1029/92WR01756.

Bolster D, Valdés-Parada FJ, LeBorgne T, Dentz M, Carrera J. 2011. Mixing in confined stratified aquifers. *Journal of Contaminant Hydrology* **120–121**: 198–212. DOI: 10.1016/j.jconhyd.2010.02.003.

Chao HC, Rajaram H, Illangasekare T. 2000. Intermediate-scale experiments and numerical simulations of transport under radial flow in a two-dimensional heterogeneous porous medium. *Water Resources Research* **36**: 2869–2884. DOI: 10.1029/2000WR900096.

Citarella D, Cupola F, Tanda MG, Zanini A. 2015. Evaluation of dispersivity coefficients by means of a laboratory image analysis. *Journal of Contaminant Hydrology* **172**: 10–23. DOI: 10.1016/j.jconhyd.2014.11.001.

Dagan G. 1984. Solute transport in heterogeneous porous formations. *Journal of Fluid Mechanics* **145**: 151–177. DOI: 10.1017/S0022112084002858.

Danquigny C, Ackerer P, Carlier JP. 2004. Laboratory tracer tests on three-dimensional reconstructed heterogeneous porous media. *Journal of Hydrology* **294**: 196–212. DOI: 10.1016/j.jhydrol.2004.02.008.

Fernàndez-Garcia D, Gómez-Hernández JJ. 2007. Impact of upscaling on solute transport: Traveltimes, scale dependence of dispersivity, and propagation of uncertainty. *Water Resources Research* **43**: W02423. DOI: 10.1029/2005WR004727.

Fernàndez-Garcia D, Sánchez-Vila X, Illangasekare TH. 2002. Convergent-flow tracer tests in heterogeneous media: combined experimental-numerical analysis for determination of equivalent transport parameters. *Journal of Contaminant Hydrology* **57**: 129–145. DOI: 10.1016/S0169-7722(01)00214-5.

Fernàndez-Garcia D, Illangasekare TH, Rajaram H. 2005a. Differences in the scale-dependence of dispersivity estimated from temporal and spatial moments in chemically and physically heterogeneous porous media. *Advances in Water Resources* **28**: 745–759. DOI: 10.1016/j.advwatres.2004.12.011.

Fernàndez-Garcia D, Rajaram H, Illangasekare TH. 2005b. Assessment of the predictive capabilities of stochastic theories in a three-dimensional laboratory test aquifer: Effective hydraulic conductivity and temporal moments of breakthrough curves. *Water Resources Research* **41**: W04002. DOI: 10.1029/2004WR003523.

Fiori A, Boso F, de Barros FPJ, Bartolo SD, Frampton A, Severino G, Suweis S, Dagan G. 2010. An indirect assessment on the impact of connectivity of conductivity classes upon longitudinal asymptotic macrodispersivity. *Water Resources Research* **46**: W08601. DOI: 10.1029/2009WR008590.

Flury M, Flühler H. 1994. Brilliant blue FCF as a dye tracer for solute transport studies – a toxicological overview. *Journal of Environmental Quality* **23**: 1108–1112. DOI: 10.2134/jeq1994.00472425002300050037x.

Freyberg DL. 1986. A natural gradient experiment on solute transport in a sand aquifer: 2. Spatial moments and the advection and dispersion of nonreactive tracers. *Water Resources Research* **22**: 2031–2046. DOI: 10.1029/WR022i013p02031.

Gelhar LW, Axness CL. 1983. Three-dimensional stochastic anal-

ysis of macrodispersion in aquifers. *Water Resources Research* **19**: 161–180. DOI: 10.1029/WR019i001p00161.

Gelhar LW, Gutjahr AL, Naff RL. 1979. Stochastic analysis of macrodispersion in a stratified aquifer. *Water Resources Research* **15**: 1387–1397. DOI: 10.1029/WR015i006p01387.

Gelhar LW, Welty C, Rehfeldt KR. 1992. A critical review of data on field-scale dispersion in aquifers. *Water Resources Research* **28**: 1955–1974. DOI: 10.1029/92WR00607.

Güven O, Molz FJ, Melville JG. 1984. An analysis of dispersion in a stratified aquifer. *Water Resources Research* **20**: 1337–1354. DOI: 10.1029/WR020i010p01337.

Heidari P, Li L. 2014. Solute transport in low-heterogeneity sandboxes: The role of correlation length and permeability variance. *Water Resources Research* **50**: 8240–8264. DOI: 10.1002/2013WR014654.

Inoue K, Kurasawa T, Tanaka T. 2016a. Quantification of macrodispersion in laboratory-scale heterogeneous porous formations. *International Journal of GEOMATE* **10**: 1854–1861. DOI: 10.21660/2016.21.5163.

Inoue K, Kurasawa T, Tanaka T. 2016b. Spatial and temporal moment approaches to quantify laboratory-scale macrodispersion in stratified porous formations. *Journal of Rainwater Catchment Systems* **22**: 15–22. DOI: 10.7132/jrcsa.22_1_15.

Jaeger S, Ehni M, Eberhardt C, Rolle M, Grathwohl P, Gauglitz G. 2009. CCD camera image analysis for mapping solute concentrations in saturated porous media. *Analytical and Bioanalytical Chemistry* **395**: 1867–1876. DOI: 10.1007/s00216-009-2978-3.

Kurasawa T, Inoue K. 2019. Effects of upscaling of physically heterogeneous porous media on solute macrodispersion phenomena. *Journal of Japan Society of Civil Engineers, Ser. A2 (Applied Mechanics (AM))* **75**: I_93–I_104 (in Japanese with English summary). DOI: 10.2208/jscejam.75.2_I_93.

Levy M, Berkowitz B. 2003. Measurement and analysis of non-Fickian dispersion in heterogeneous porous media. *Journal of Contaminant Hydrology* **64**: 203–226. DOI: 10.1016/S0169-7722(02)00204-8.

Mackay DM, Freyberg DL, Roberts PV, Cherry JA. 1986. A natural gradient experiment on solute transport in a sand aquifer: 1. Approach and overview of plume movement. *Water Resources Research* **22**: 2017–2029. DOI: 10.1029/WR022i013p02017.

McNeil JD, Oldenborger GA, Schincariol RA. 2006. Quantitative imaging of contaminant distributions in heterogeneous porous media laboratory experiments. *Journal of Contaminant Hydrology* **84**: 36–54. DOI: 10.1016/j.jconhyd.2005.12.005.

Mercado A. 1967. Spreading pattern of injected water in a permeability stratified aquifer. *Proceedings of Symposium of Haifa, Artificial Recharge and Management of Aquifers, International Association of Hydrological Sciences Publication* **72**: 23–36.

Nakagawa K, Saito M, Berndtsson R. 2012. On the importance of hysteresis and heterogeneity in the numerical simulation of unsaturated flow. *Hydrological Research Letters* **6**: 59–64. DOI: 10.3178/HRL.6.59.

Pickens JF, Grisak GE. 1981. Scale-dependent dispersion in a stratified granular aquifer. *Water Resources Research* **17**: 1191–1211. DOI: 10.1029/WR017i004p01191.

Silliman SE, Simpson ES. 1987. Laboratory evidence of the scale effect in dispersion of solutes in porous media. *Water Resources Research* **23**: 1667–1673. DOI: 10.1029/WR023i008p01667.

Sudicky EA. 1986. A natural gradient experiment on solute transport in a sand aquifer: Spatial variability of hydraulic conductivity and its role in the dispersion process. *Water Resources Research* **22**: 2069–2082. DOI: 10.1029/WR022i013p02069.

Ursino N, Gimmi T, Flühler H. 2001. Combined effects of heterogeneity, anisotropy, and saturation on steady state flow and transport: A laboratory sand tank experiment. *Water Resources Research* **37**: 201–208. DOI: 10.1029/2000WR900293.

Ye Y, Chiogna G, Cirpka OA, Grathwohl P, Rolle M. 2015. Experimental evidence of helical flow in porous media. *Physical Review Letters* **115**: 194502. DOI: 10.1103/PhysRevLett.115.194502.

Zavala-Sanchez V, Dentz M, Sanchez-Vila X. 2009. Characterization of mixing and spreading in a bounded stratified medium. *Advances in Water Resources* **32**: 635–648. DOI: 10.1016/j.advwatres.2008.05.003.

Zhang C, Suekane T, Minokawa K, Hu Y, Patmonoaji A. 2019. Solute transport in porous media studied by lattice Boltzmann simulations at pore scale and x-ray tomography experiments. *Physical Review E* **100**: 063110. DOI: 10.1103/PhysRevE.100.063110.

Zinn B, Meigs LC, Harvey CF, Haggerty R, Peplinski WJ, Von Schwerin CF. 2004. Experimental visualization of solute transport and mass transfer processes in two-dimensional conductivity fields with connected regions of high conductivity. *Environmental Science & Technology* **38**: 3916–3926. DOI: 10.1021/es034958g.